Effect of the oxidation state and hydrogen concentration on the lifetime of thermally fixed holograms in $LiNbO_3$:Fe

E. M. de Miguel-Sanz
Departamento de Óptica y Optometría, Universidad Europea de Madrid, Villaviciosa de Odón, Madrid, Spain

M. Carrascosa and L. Arizmendi
Departamento de Física de Materiales, C-IV, Universidad Autónoma de Madrid, Cantoblanco, 28049 Madrid, Spain

(Received 24 September 2001; published 22 March 2002)

The lifetime of thermally fixed holograms in iron-doped lithium niobate is extensively studied for samples with different iron oxidation state and hydrogen concentrations. The results clearly follow the theoretically predicted relationship of the lifetime of fixed holograms with these parameters. This undoubtedly proves that only protons are the ionic charge carriers responsible for thermal fixing in these crystals. From these measurements of lifetimes at different temperatures under uniform illumination, the diffusion coefficient for protons is determined to be $D_h=(1.4\times10^{-3}\ \mathrm{cm^2\,s^{-1}})\exp[-(0.95\ \mathrm{eV})/k_BT]$.

DOI: 10.1103/PhysRevB.65.165101 PACS number(s): 42.40.Eq, 42.40.Lx, 42.70.Nq

I. INTRODUCTION

Recently there has been an increasing interest in the use of stable volume holograms for different applications, e.g., narrow-band optical filters,[1] diffractive devices,[2] optical memories,[3–5] optical correlators,[6] and dense wavelength-division multiplexing demultiplexers.[7] This is mainly due to the recent improvements in the fixing technique knowledge,[8–11] now giving the possibility of producing stable, optically nonerasable, holograms of very high diffraction efficiency (close to 100%) in $LiNbO_3$ crystals.[9] Such a high diffraction efficiency can be achieved in a sample of less than 1 mm thick. This means that this material can support fixed holographic gratings of relatively high refractive index change compared with other photorefractive materials in which thermal fixing has been observed [$BaTiO_3$,[12] $KNbO_3$,[13] KTN,[14] BSO,[15] and $La_3Ga_5SiO_{14}$:Pr^{3+} (Ref. 16)]. The reason for this higher diffraction efficiency is known at the present time to be due to the role of the high photovoltaic constant of Fe in lithium niobate in developing of the holograms.[11,17]

The thermal fixing procedure basically consists of transforming the light-erasable trapped charge pattern, responsible for the standard photorefractive effect, into a fixed (light-insensitive) matched pattern. Then damage of the stored information during readout is avoided. This effect was discovered in 1971 by Amodei and Staebler.[18] The complete thermal fixing process includes two steps. First, during or after recording, the sample is heated to temperatures in the 120–180 °C range. At these temperatures, H^+ ions present in the sample move to form a grating that neutralizes the former electronic trapped charge grating. This step is called ''fixing'' throughout this paper. The first evidence of hydrogen redistribution in a $LiNbO_3$ crystal illuminated by a macroscopic light beam at high temperature (160°) was reported by Vormann *et al.*[19] in 1981. More recently Buse *et al.*[20] demonstrated that a macroscopic impurity valence distribution induced by a light beam is compensated by a H^+ redistribution after heating the sample at about 160 °C. These works pointed out that hydrogen is an impurity responsible for fixing in $LiNbO_3$. In a second step the hologram is developed by using homogeneous illumination at lower temperature, at which the ionic grating is frozen, acting on the electronic grating. The result of this process is to recover the diffraction efficiency partially. We will refer to this process as ''developing the hologram.'' The diffraction efficiency observed after this step is produced by the resulting grating. This is the superposition of the ionic grating, produced by the fixing process, and a part of the initial electronic one. The electronic grating is decreased and, which is more important, shifted by the homogeneous illumination of developing.[11] The role of the high photovoltaic effect exhibited by Fe in lithium niobate is absolutely fundamental for highly developed diffraction efficiency in relatively thin samples.

Another method by which to obtain long lasting holograms insensitive to the reading light in $LiNbO_3$, is based on multiphoton recording, using one-color light nonlinear effects or two-color light. It was discovered in 1974,[21] and extensively studied (see Ref. 22, and references therein). In the case of two-color holography, the sensitizing light of shorter wavelength promotes the electronic charges from deep traps to shallow ones, and light of longer wavelength (usually in the near IR) is used for recording. Then, using only reading light at the recording wavelength, the stored hologram is not appreciably erased. The holograms can be optically erased by the shorter wavelength light. Compared with thermal fixing, the advantages of this method are that it is all optical and near-infrared coherent light can be used for recording. In contrast, the main disadvantages are the lower maximum diffraction efficiencies and dark decays of the order of several months,[22] much shorter than in thermal fixed holograms. Recent studies showed that dark decay times can be enlarged using a second dopant which introduces deep traps in the material.[23,24] In any event, two-color recording seems to be more useful for holographic memories, whereas thermal fixing could be more convenient for single diffractive devices. In any case, thermal fixing and two-color recording are not opposite techniques, and could be combined for mutual benefit.

TABLE I. Sample characteristics.

	$\alpha_{477\,\mathrm{nm}}$ (cm^{-1})	$[Fe^{2+}]/[Fe^{3+}]$	N_t (cm^{-3})	$\alpha_{2870\,\mathrm{nm}}$ (cm^{-1})	$[H_0]$ (cm^{-3})
Sample No. 1	3.5	0.045	7.4×10^{17}	1.6	1.7×10^{19}
Sample No. 2	2.9	0.037	6.1×10^{17}	0.32	3.4×10^{18}
Sample No. 3	0.45	0.0056	9.8×10^{16}	2.94	3.13×10^{19}

The purpose of the present work is to study the effect of the oxidation state of the photorefractive impurity and of the concentration of hydrogen on the lifetimes of fixed holograms. In this study we will determine the optimum crystal conditions to obtain fixed holograms with the longest possible lifetimes and the highest diffraction efficiencies to be useful for practical applications. It was recently determined that the oxidation state of the samples, i.e., the Fe^{3+}/Fe^{2+} ratio, influences the fraction of the initial hologram that can be developed, and hence the final diffraction efficiency.[11] For a given total dopant amount, the more oxidized crystals (with low $[Fe^{3+}/Fe^{2+}]$ ratio) give relatively more highly developed holograms. On the other hand, the theoretical predictions show dependence of the decay time of fixed holograms on both the oxidation state and the hydroxyl concentration.[8,25] By means of thermal treatments in the proper atmosphere, it is possible to act on the oxidation state of iron ions and on the total OH^- content of the samples. We have carried out measurements of fixed hologram diffraction decays at different temperatures and for different sample characteristics.

II. EXPERIMENT

The samples used in our experiments were obtained from lithium niobate crystals grown from a congruent melt doped with 0.1 mol % of iron. From them samples of $10\times9\times1.3\,\mathrm{mm}^3$, with the crystallographic *c* axis laying on the larger faces, were sawn and polished up to obtain optical quality surfaces.

Different reduction states and/or different OH^- concentrations were achieved by undergoing the samples to oxidation/reduction thermal treatments in proper atmospheres. Sample No. 1 is from the as-grown crystal. Sample No. 2 is from the same boule but it was first treated in dry oxygen at 800 °C for 2 h to reduce the hydrogen content, and subsequently to a slight reduction treatment at 500 °C in a vacuum to restore approximately the initial iron oxidation state. Finally, sample No. 3 was strongly oxidized in wet oxygen at 900 °C for 3 h.

The iron oxidation state and the OH^- content of the samples were checked by measuring their optical absorption at 477 and 2870 nm, respectively. The reduction state of the samples was estimated from the absorption coefficient at 477 nm with the absorption cross-section parameter for the Fe^{2+} band,[26] and assuming that the total iron concentration in the samples was about 0.09 mol % due to an iron segregation coefficient slightly smaller than 1.[27] The hydrogen concentration was estimated from the absorption coefficient of the OH^- stretching band at 2870 nm and the corresponding cross section.[28] The obtained values of these parameters for the three samples are summarized in Table I. It should be noted that for all samples the amount of hydrogen is well higher than the amount of Fe^{2+} ions, so in all cases there is enough hydrogen for a full compensation of the hologram gratings during the fixing process.

The holograms were recorded using a two-beam coupling configuration with an Ar^+ laser at 514.5 nm. Both writing beams were expanded to illuminate the entire sample. The crossing beam half-angle set in this work to 14.9° in order to have holograms with a grating spacing of 1.0 μm. To avoid the spatial charge accumulation due to the photovoltaic effect exhibited by the lithium niobate crystals under illumination, the samples were short circuited by covering their four lateral faces with conductive silver paste. In this setup the sample was oriented with its *c* axis parallel to the face and lying in the incidence plane. A He-Ne laser beam of very low power, impinging on the sample at its Bragg angle, was used as a probe. The diffracted part of this beam was continuously monitored.

For the recording and fixing of holograms, the sample was mounted in a holder placed inside a vacuum chamber provided with large optical windows. The temperature of the sample could be changed between 20 and 300 °C by means of a small heating element in contact with the holder. A thermocouple was used to measure the temperature continuously. Temperature control with a precision of ±0.1 °C was achieved by an Eurothem 818 Temperature Controller/Programmer. With this system the holograms could be thermally fixed either during or after recording. Optical development of fixed holograms was produced by illuminating both sides of the sample with the white light of two 150-W halogen tungsten lamps focused on the surfaces. Both faces of the sample were illuminated totally during the developing as well as during all the decay process. Absorption of this light by the samples resulted in an increase of temperature of less than 5 °C in all cases, and they reached a stable level in about 5 min.

III. RESULTS AND DISCUSSION

The time evolution of the diffraction efficiency of holograms of 1-μm fringe spacing was measured under white-light illumination for a long time at different constant temperatures. These measurements were done in the three different samples presented in Sec. II. The signal decays obtained resulted in all cases to be pure single-exponential time dependencies without any constant background. For each sample a higher temperature resulted in a faster decay. These facts inform us that the decays are due to a single thermally activated process.

Figure 1 shows Arrhenius-like plots of the exponential

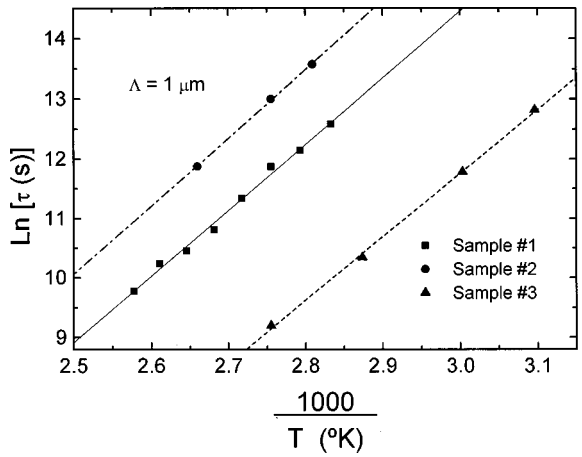

FIG. 1. Arrhenius-like plot of the lifetime of fixed holograms of 1-μm grating spacing at different temperatures for the three different samples. Full squares, circles, and triangles correspond to values derived from the experimental decays. The values obtained for each sample were fitted to a straight line.

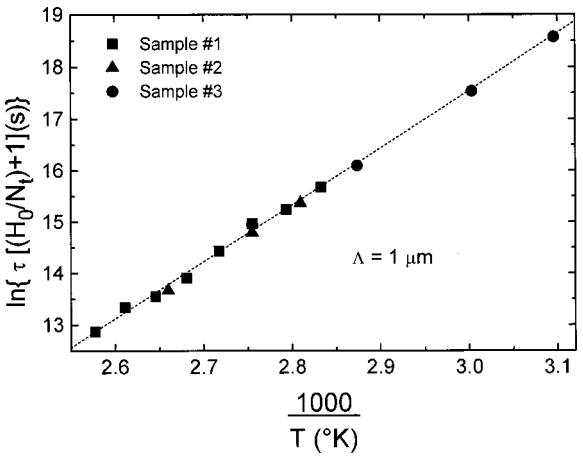

FIG. 2. Plot of the lifetime values multiplied by the corresponding $[(H_0/N_t)+1]$ factor for each sample vs the inverse absolute temperature of acquisition.

decay time factors. For each sample the points appear aligned in a straight-line dependence. Furthermore, the lines corresponding to the three samples appear parallel to the others, announcing that the processes involved in the decays have the same activation energy but different preexponential factor for different samples. From the common slope we have determined an activation energy of $E_a=0.95 \pm 0.02$ eV. Later we will discuss this value in comparison with other values found in the literature. As the differences among the samples are their oxidation state and hydrogen concentration, it is also evident from Fig. 1 that these characteristics influence the lifetime of the fixed holograms.

A. Comparison with the theory

We will consider the theory for high-temperature photorefractive phenomena in lithium niobate crystals, derived by Sturman *et al.*,[25] for electrons and protons as charge carriers in this material. According to this theory, the thermally activated kinetics of the electric-field amplitude of a holographic grating at a given temperature is complex. The time evolutions in the dark as well as under uniform illumination are in general a linear combination of two exponentials whose characteristic rate constants are due in a mixed way to electron and proton diffusion. Only in particular situations can these time constants be attributed separately to diffusion of one of the charged species. In our situation of intense illumination we are in the approach of fast rising time process of developing and a subsequent slow decay. The constant rate for the fast developing is just the dielectric relaxation rate of electrons, $\Gamma_f \cong \gamma_e^{\mathrm{ph}}=e\mu_e\sigma I_0 N_D/\varepsilon\varepsilon_0\gamma N_A$, where e is the electron charge, μ_e is the electronic mobility, σ is the photoionization cross section, I_0 is the light intensity of active wavelength, N_D and N_A are the concentrations of donors and acceptors, respectively, γ is the trapping coefficient, and $\varepsilon\varepsilon_0$ is the dielectric permittivity of the material. This rate constant is related to the photoexcited charge carriers. Because this rate is proportional to the intensity of developing light, and in our case this is of the order of 140 mW/cm^2, the developing is done in a short initial time, very fast compared with the decay times, as we observed experimentally. In fact, even for the highest temperatures used in our experiments, the white-light intensity provided by our lamps was always high enough to fully develop the holograms in a much shorter time. So the subsequent slow decay, that is what we measured precisely, is already a single exponential.

In this situation of strong uniform illumination, the observed slow time decay has a constant rate $\Gamma_s'=\gamma_h R_d^2 K^2(1+N_t/H_0)$, where $\gamma_h=e\mu_h H_0/\varepsilon\varepsilon_0$ is the dielectric relaxation rate of protons, $R_d=(\varepsilon\varepsilon_0 k_B T/N_t e^2)^{1/2}$ is the Debye screening length, and $K=2\pi/\Lambda$ the grating spatial frequency. $N_t=N_a N_d/(N_a+N_d)$ is the effective trap density and H_0 the proton density. $\mu_h=D_h e/k_B T$ being the protonic mobility, where D_h is the diffusion coefficient of protons in lithium niobate. After substitution, we can easily write the slow rate in the form

$$\Gamma_s'=\frac{1}{\tau}=D_h K^2\left[\frac{H_0}{N_t}+1\right]. \tag{1}$$

The thermal dependence comes from the diffusion coefficient D_h in the form

$$D_h=D_h^0\cdot\exp(-E_a/k_B T). \tag{2}$$

Note that in this expression the activation energy E_a corresponds purely to the hydrogen diffusion (ε_h in Ref. 25), and not to a mixed energy due to activation of electrons and protons.

In order to check the validity of the theoretical dependence given in expression (1), in Fig. 2 we draw an Arrhenius-like plot of the product of the lifetime values by the factor $[(H_0/N_t)+1]$ that characterizes each sample. The result is that all points measured for the different samples fall along the same straight line. This result confirms the theoretically predicted dependence on H_0/N_t and the temperature.

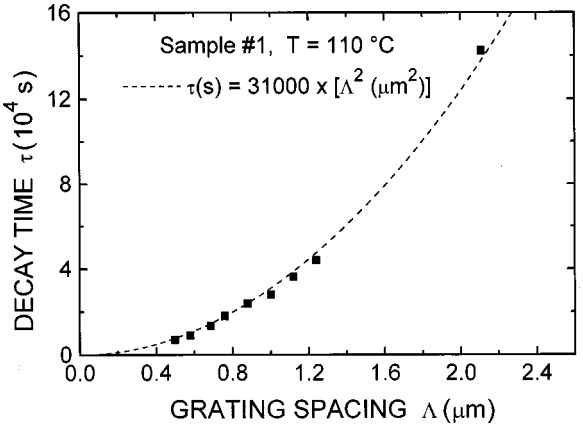

FIG. 3. Plot of the lifetime values for holograms with different fringe spacing at 110 °C for sample No. 1 vs the spatial frequency *K*.

In the literature there is a dispersion of values of the hydrogen absorption cross section obtained by different techniques. The authors of Ref. 29, using nuclear magnetic resonance measurements, obtained a value of $\sigma_{OH}=(3.3\pm1.1)\times10^{-20}$ cm^2, which is the lowest reported value. Kovács *et al.*[30] determined a value of $\sigma_{OH}=(6\pm3.8)\times10^{-20}$ cm^2 by atomic absorption spectroscopy. From photorefractive fixing was also possible to obtain this constant, giving a value of $\sigma_{OH}=(9.4\pm1.6)\times10^{-20}$ cm^2,[28] this being the value we consider in our calculation of the hydrogen diffusion coefficient because it is determined with the same kind of average of hydrogen situations inside the crystal. Other published values are $\sigma_{OH}=(40\pm20)\times10^{-20}$ cm^2, determined by Richter *et al.*[31] using secondary-ion-mass spectroscopy, and $\sigma_{OH}=(41.5\pm6)\times10^{-20}$ cm^2, obtained in Ref. 32 in studies of proton diffusion. These two last values were obtained for proton exchanged layers where the concentration is very high and the behavior of protons could be different. In the case of an error in the value of absorption cross section, the analysis of the results and the look of Fig. 2 are not appreciably affected. The activation energy will be the same. Only the preexponential factor could be affected.

The quadratic dependence of the slow rate on the grating spatial frequency *K* was also investigated. In Fig. 3 we present the decay rates obtained for different grating spacing at a constant temperature of 110 °C, plotted versus the spatial frequency. The points are very well fitted to a parabolic curve passing by zero.

Thus we have proved that our samples fulfill the predicted dependence of the slow decay rate on the effective trap concentration N_t, on the proton concentration H_0, as well as on the spatial frequency *K*. This confirms the validity of the theoretical frame for the case of our samples.

B. Proton diffusion coefficient

From the fitting of points of Fig. 2 to a straight line one obtains the value of the proton diffusion preexponential factor D_h^0, resulting in this case a value of $(1.4\pm0.5)\times10^{-3}$ cm^2 s^{-1}. Thus, we can say that the diffusion coefficient of hydrogen in lithium niobate is

$$D_h=[(1.4\pm0.5)\times10^{-3}\ \text{cm}^2\,\text{s}^{-1}]\times\exp[-(0.95\pm0.02\ \text{eV})/k_BT]. \quad (3)$$

We want to remark here that with this method to obtain the diffusion coefficient for hydrogen in lithium niobate, we access the value for bulk diffusion. This is because the grating planes are distributed all over the bulk, and their decay is driven by the average diffusion in all the volume, where the volume occupied by dislocations or other defects that could alter the diffusion is of small importance.

C. Comparison of activation energies and preexponential factors

In respect of the activation energy, there is some discrepancy among the different reported values.[33] We will consider only those measured optically in processes related with hologram fixing in the bulk. Other techniques such as macroscopic proton diffusion can receive a contribution of conductivity along dislocations or other defects. The authors of Ref. 34 gave a value of $E_a=1.03\pm0.02$ eV in an experiment similar to the one presented here, but with the difference that in the former work the crystal was illuminated during decays with a coherent beam, which formed, with its internal reflected part, some interference fringes inside the sample, leading to a spatial intensity variation and to irregular illumination. Now we illuminate the sample with incoherent white light from both faces.

Other reported decay measurements are done under dark conditions. One of these measurements is the decay of the developed hologram in the dark at temperatures in the range 70–120 °C.[34] In this case the decays have to be interpreted, after the theoretical study of Ref. 25, as due to the movement of the ionic grating to compensate the shifted electronic grating. These decays were in most cases faster than decays under illumination, and did not depend on the grating spacing. They could not be fitted only to one exponential without background. A reanalysis of data presented in Ref. 34 to double-exponential decays resulted in a fast decay independent of *K* and a very slow decay with time constant depending on the grating period. The analysis of the thermal dependence of the fast decay resulted in an activation energy of 1.13 ± 0.1 eV.

Other very recent dark measurements are those from Ellabban *et al.*,[35] corresponding to the fixing compensation of the electronic scattering gratings by protons at different temperatures in $LiNbO_3$:Mn (0.1 mol %). They obtained a value of $E_a=1.05\pm0.03$ eV.

Yang *et al.*[36] also carried out temperature dependence measurements of dark decay experiments in lithium niobate crystals with different stoichiometries and doped with different amounts of iron. In highly doped samples they found an activation energy of 0.28 eV which has been attributed to electron tunneling between adjacent iron ions.[37] But for samples with an iron concentration of 2×10^{19} cm^{-3} or lower (as in our case) they found activation energies in the range 1.1–0.97 eV. They also observed a transition concentration region with double exponentials in which both activation energies are detected. It is worth remarking that for

our samples of 1.8×10^{19}-cm^{-3} iron doping, we did not observe any tunneling contribution.

We do not have a fully satisfactory explanation for the moderate differences of the proton activation energy obtained here in comparison with those of dark decays, although we would have some further comments. The theory developed by Sturman *et al.*[25] predicted, for dark decays in the approximation of mobility of protons much greater than that for thermally excited electrons, a double-exponential decay. In this case the fast decay rate is $\Gamma_f \approx \gamma_h = e\mu_h H_0/\epsilon\epsilon_0 = e^2 D_h H_0/k_B T\varepsilon\varepsilon_0$, insensitive to the grating spacing and to the thermal activation of the diffusion of protons. The slow decay rate is now $\Gamma_s \cong \gamma_e^T K^2 R_d^2(1+N_t/H_0)$, where $\gamma_e^T = e\mu_e n_0^T/\varepsilon\varepsilon_0$ is the dielectric relaxation rate of thermally activated electrons. This latter rate is very small at the temperature range of measurement in Refs. 33–35, and this second decay could be taken into account in the analysis as a constant background. If this term is not introduced, there could be some imprecision in the determination of activation energy of the fast decay. In our opinion the dark decays have certain difficulties for data analysis. Ellabban *et al.*[35] measured the scattering using a weak beam of 488-nm wavelength. This wavelength is very active for excitation of electronic charges in doped lithium niobate, and can also affect the results. Furthermore, these authors did not consider the existence of a second decay rate, slower in this case. In the same sense, the dark decays of Ref. 34 could not be fitted to single exponentials, and this probably introduces some uncontrolled error in the fitting. By contrast, the decays of the present paper, being (and predicted to be) single exponential, seem more adequate to determine this activation energy.

There is also some spread of diffusion coefficient preexponential factor values in the literature. Kovacs *et al.*[38] measured a value of 0.1 cm^2/s, whereas other authors[39] reported values of the order of 0.035 cm^2/s. The lowest reported value was 5.1×10^{-3} cm^2/s, measured by Clark *et al.*[40] in proton-exchanged lithium niobate. The value obtained in the present paper (3) is even lower. However, we have checked that our experimental results of Fig. 2 are not compatible with higher values of D_h^0. For comparison, in TiO_2 it was found[41] that there is an anisotropic coefficient, with $D_h^0 = 3.8\times10^{-1}$ cm^2/s for diffusion perpendicular to the *c* axis, and more than two orders of magnitude less, $D_h^0 = 1.8\times10^{-3}$ cm^2/s, for diffusion parallel to the *c* axis. As in lithium niobate, in this crystal the OH stretching infrared absorption band is also totally σ polarized. A similar diffusion anisotropy could explain the dispersion of values found in lithium niobate as well as our low value because, in our case, due to the grating orientation, the erasure of the ionic gratings have to be produced by diffusion in direction of the *c* axis.

D. Fixed holograms for practical devices

From our present study we know how the oxidation state and the hydrogen concentration of the crystal influence the lifetime of fixed holograms. Long-lasting fixed holograms are those with larger values of τ. According to Eq. (1), the largest τ values, for a given grating frequency *K* and assuming a hydrogen diffusion coefficient D_h independent of hydrogen concentration, are obtained for low proton concentration (small H_0) and large effective trap concentration N_t. So, there is a theoretical limit for the decay time constant of a hologram of a given grating spacing. This is obtained when the ratio $H_0/N_t \ll 1$ and can be neglected in Eq. (1). In fact the limit decay times will correspond to those values plotted in Fig. 2. Note that the magnitude of the vertical axis in this figure is actually the limit time coefficient $\tau_{\max} = 1/D_h K^2$.

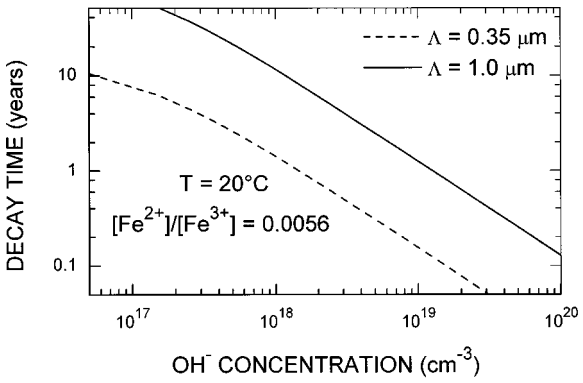

FIG. 4. Calculated decay times for holograms of 1- and 0.35-μm spacings at 20 °C using the OH^- diffusion coefficient obtained, as a function of the OH^- concentration in the crystal. This is done assuming the oxidation state of sample No. 3.

In practice, if one wants to obtain a long-lasting fixed hologram, the crystal must have low hydrogen concentration and a relatively high effective trap concentration. Using the diffusion coefficient obtained, in Fig. 4 we plot an estimation of the lifetimes at room temperature (20 °C) for holograms with 1- and 0.35-μm grating spacings, assuming the oxidation state of our sample No. 3, as a function of the hydrogen concentration in the sample. We chose a 0.35-μm grating spacing because this is the required spacing for backreflection in this material of light with a wavelength of 1550 nm. As one can see in the figure, in spite of the lower lifetimes obtained for small spacings, interesting lifetimes of several years could be achieved by reducing the hydrogen concentration. This can be done by thermal treatments in dry oxygen atmosphere, and concentrations as low as 3×10^{17} cm^{-3} can easily be obtained in this way. We have elected to present this figure for a more oxidized sample, in spite of its lower N_t, and consequently lower lifetimes, because of the more highly developed field ratio exhibited by the more oxidized samples.[11] Because of the soft variation of the developed field ratio with the oxidation state, one could choose a less oxidized sample, sacrificing a little the developed field ratio in order to obtain much longer lifetimes than those presented in Fig. 4.

Note that Fig. 4 is plotted for holograms kept under intense illumination during all its life. If this is not done, the hologram experiences a dark decay whose fast component is independent of the grating spacing. The room-temperature decay time can be extrapolated from high-temperature data. Using the measurements presented in Ref. 11 we get obtain a value of 2.1 years for this dark decay. Thus the hologram could not be continuously illuminated with visible light be-

cause this decay is slow enough. Moreover, a hologram that has experienced this decay in the dark can recover most of its initial diffraction efficiency with intense visible illumination during a short time, e.g., 1 h. A schedule of short-period illumination, for example each half a year, is sufficient to keep the fixed hologram at a diffraction efficiency close to its highest initial value. In fact, the true grating decay in the dark, not retrievable by further developing, is slower than that experienced under continuous illumination. In this sense dark lifetimes would be longer than our presented decays under illumination.

IV. CONCLUSIONS

Our experimental analysis of the hologram's lifetime dependence on OH^- concentration, the oxidation state of the samples, and the grating spacing shows that the samples follow the theoretically predicted behavior very well. In particular, the decay rate dependence on the hydrogen concentration is a decisive proof that these ions are the exclusive charge species responsible for thermal fixing in our crystals. From these data we have obtained the value of diffusion coefficient and its activation energy for hydrogen diffusion in the bulk material.

Our results show that a high diffraction efficiency, close to 100%, and a sufficiently long lifetime can be achieved together in a practical $LiNbO_3$:Fe crystal. As we demonstrated, this is obtained for oxidized samples having a low hydrogen concentration. Taking our present study into account, it is possible to tailor a sample with optimum properties for practical holographic devices. In particular, in Sec. III we have estimated the lifetime of a fixed holographic Bragg reflector for operation at the wavelengths of the third optical communications window. In spite of the low grating spacing in this system, it is possible to obtain a device lifetime of the order of ten years.

ACKNOWLEDGMENTS

We wish to acknowledge financial support from the Spanish Ministerio de Educación y Cultura (Grant Nos. PB97-0008 and PB98-0056) and Comunidad de Madrid (Grant No. 07T/0043/2000).

[1] G. Barbastathis, M. Balberg, and D. J. Brady, Opt. Lett. **24**, 811 (1999).
[2] S. Breer and K. Buse, Appl. Phys. B: Photophys. Laser Chem. **66**, 339 (1998).
[3] X. An, D. Psaltis, and G. W. Burr, Appl. Opt. **38**, 386 (1999).
[4] J. F. Heanue, M. C. Bashaw, A. J. Daiber, R. Snyder, and L. Hesselink, Opt. Lett. **21**, 1615 (1996).
[5] S. Bains, Opt. Photonics News **11**, 36 (2000).
[6] E. M. de Miguel-Sanz, M. Tebaldi, S. Granieri, N. Bolognini, and L. Arizmendi, Appl. Phys. B: Photophys. Laser Chem. **70**, 279 (2000).
[7] S. Breer, H. Vogt, I. Nee, and K. Buse, Electron. Lett. **34**, 2419 (1998).
[8] L. Arizmendi, E. M. de Miguel-Sanz, and M. Carrascosa, Opt. Lett. **23**, 960 (1998).
[9] A. Mendez and L. Arizmendi, Opt. Mater. **10**, 55 (1998).
[10] C. R. Hsieh, S. H. Lin, K. Y. Hsu, T. C. Hsieh, A. Chiou and J. Hong, Appl. Opt. **38**, 6141 (1999).
[11] E. M. de Miguel, J. Limeres, M. Carrascosa and L. Arizmendi, J. Opt. Soc. Am. B **17**, 1140 (2000).
[12] D. Kirillov and J. Feinberg, Opt. Lett. **16**, 1520 (1991).
[13] G. Montemezzani and P. Günter, J. Opt. Soc. Am. B **7**, 2323 (1990).
[14] T. Imai, S. Yagi, and H. Yamazaki, J. Opt. Soc. Am. B **13**, 2524 (1996).
[15] L. Arizmendi, J. Appl. Phys. **65**, 423 (1988).
[16] T. Nikolajsen and P. M. Johansen, Opt. Lett. **24**, 1419 (1999).
[17] M. Carrascosa and F. Agulló-López, Opt. Commun. **126**, 240 (1996).
[18] J. J. Amodei and D. L. Staebler, Appl. Phys. Lett. **18**, 540 (1971).
[19] H. Vormann, G. Weber, S. Kapphan, and E. Krätzig, Solid State Commun. **40**, 543 (1981).
[20] K. Buse, S. Breer, K. Peithmann, M. Gao, and E. Krätzig, Phys. Rev. B **56**, 1225 (1997).
[21] D. von der Linde, A. M. Glass, and K. F. Rodgers, Appl. Phys. Lett. **25**, 155 (1974).
[22] H. Guenther, R. Macfarlane, Y. Furukawa, K. Kitamura, and R. Neurgaonkar, Appl. Opt. **37**, 7611 (1998).
[23] A. Adibi, K. Buse, and D. Psaltis, J. Opt. Soc. Am. B **18**, 584 (2001).
[24] H. Hatano, S. Tanaka, T. Yamaji, M. Lee, S. Takekawa, and K. Kitamura, in *Photorefractive Effects, Materials, and Devices*, 2001 TOPS, Vol. 62, edited by D. Nolte (OSA, Washington, D.C., 2001), p. 171.
[25] B. I. Sturman, M. Carrascosa, F. Agulló-López, and J. Limeres, Phys. Rev. B **57**, 12 792 (1998).
[26] H. Kurz, E. Krätzig, W. Keune, H. Engelman, U. Gonser, B. Dischler, and A. Rauber, J. Appl. Phys. **12**, 355 (1977).
[27] A. Rauber, in *Chemistry and Physics of Lithium Niobate*, edited by E. Kaldis, Current Topics in Materials Science Vol. 1 (North-Holland, Amsterdam, 1978), p. 481.
[28] R. Müller, L. Arizmendi, M. Carrascosa, and J. M. Cabrera, Appl. Phys. Lett. **60**, 3212 (1992).
[29] W. Bollmann, K. Schlothauer, and J. Zogal, Krystall. und Thechnik **11**, 1327 (1976).
[30] L. Kovács, Zs. Szaller, I. Cravero, and C. Zaldo, J. Phys. Chem. Solids **51**, 417 (1990).
[31] R. Richter, T. Bremer, P. Hertel, and E. Krätzig, Phys. Status Solidi A **114**, 765 (1989).
[32] S. Klauer, M. Wöhlecke, and S. Kapphan, Phys. Rev. B **45**, 2786 (1992).
[33] J. M. Cabrera, J. Olivares, M. Carrascosa, J. Rams, R. Müller, and E. Dieguez, Adv. Phys. **45**, 349 (1996).
[34] L. Arizmendi, A. Méndez, and J. V. Álvarez-Bravo, Appl. Phys. Lett. **70**, 571 (1997).
[35] M. A. Ellabban, G. Mandula, M. Fally, R. A. Rupp, and L. Kovàcs, Appl. Phys. Lett. **78**, 844 (2001).

[36] Y. Yang, I. Nee, K. Buse, and D. Psaltis, Appl. Phys. Lett. **78**, 4076 (2001); in *Photorefractive Effects, Materials, and Devices*, 2001 TOPS, Vol. 62, edited by D. Nolte (OSA, Washington, D.C., 2001), p. 144.

[37] I. Nee, M. Müller, K. Buse, and E. Krätzig, J. Appl. Phys. **88**, 4282 (2000).

[38] L. Kovacs, K. Polgar, R. Capelletti, and C. Mora, Phys. Status Solidi A **120**, 97 (1990).

[39] W. Bollmann and H. J. Stöhr, Phys. Status Solidi A **39**, 477 (1977).

[40] D. F. Clark, A. C. G. Nutt, K. K. Wong, P. J. R. Laybourn, and R. M. De La Rue, J. Appl. Phys. **54**, 6218 (1983).

[41] O. W. Johnson, S. H. Paek, and J. W. DeFord, J. Appl. Phys. **46**, 1026 (1975).